Short Article

Developmental Cell

Zeb Family Members and Boundary Cap Cells Underlie Developmental Plasticity of Sensory Nociceptive Neurons

Graphical Abstract

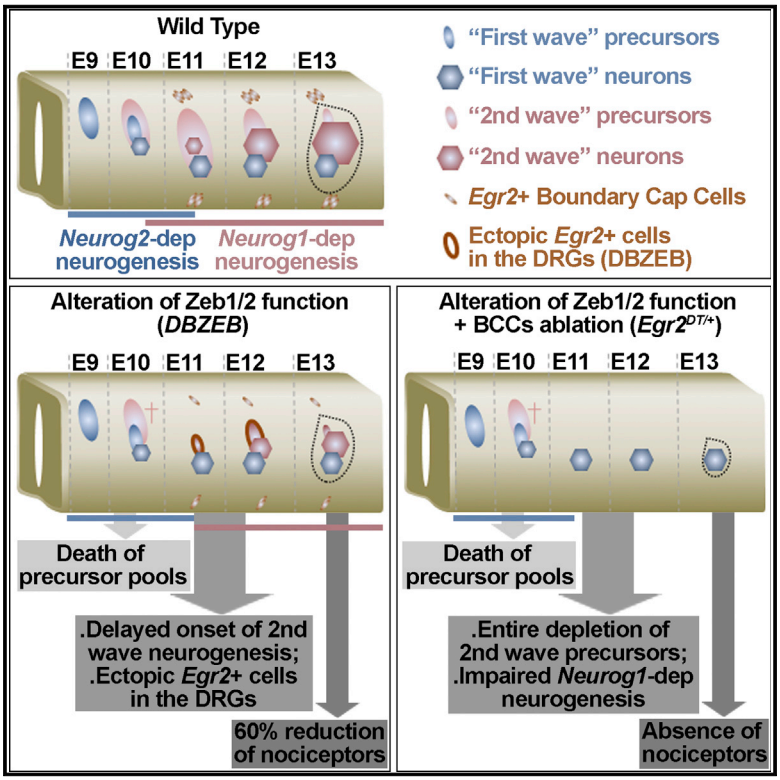

Highlights

- Zeb1/2 support survival of precursor populations generating sensory nociceptors
- *Neurog1*-dependent neurogenesis can be functionally divided in two successive phases
- Combined alteration of Zeb1/2 function and BCC ablation lead to nociceptor agenesis
- Zeb1/2 and BCCs underlie developmental plasticity of sensory nociceptive neurons

Authors

David Ohayon, Stéphanie Ventéo, ..., Patrick Carroll, Alexandre Pattyn

Correspondence

alexandre.pattyn@inserm.fr

In Brief

Ohayon et al. provide functional evidence supporting diversity among sensory precursors undergoing *Neurog1*-dependent neurogenesis and illustrate developmental plasticity in the peripheral somatosensory system. They show that combined alteration of Zeb1/2 function and boundary cap cell ablation entirely deplete nociceptive precursors, thus leading to complete agenesis of sensory nociceptors.

Ohayon et al., 2015, Developmental Cell *33*, 343–350
May 4, 2015
http://dx.doi.org/10.1016/j.devcel.2015.03.021

CellPress

Developmental Cell
Short Article

Zeb Family Members and Boundary Cap Cells Underlie Developmental Plasticity of Sensory Nociceptive Neurons

David Ohayon,[1,2] Stéphanie Ventéo,[1] Corinne Sonrier,[1] Pierre-André Lafon,[1] Alain Garcès,[1] Jean Valmier,[1,3] Cyril Rivat,[1,3] Piotr Topilko,[4] Patrick Carroll,[1] and Alexandre Pattyn[1,*]
[1]INSERM U1051, Institut des Neurosciences de Montpellier, 34091 Montpellier, France
[2]Université de Toulouse, Centre de Biologie du Développement, UMR5547 CNRS, 31062 Toulouse, France
[3]Université Montpellier 2, 34091 Montpellier, France
[4]INSERM U1024, Ecole Normale Supérieure, 75230 Paris, France
*Correspondence: alexandre.pattyn@inserm.fr
http://dx.doi.org/10.1016/j.devcel.2015.03.021

SUMMARY

Dorsal root ganglia (DRG) sensory neurons arise from heterogeneous precursors that differentiate in two neurogenic waves, respectively controlled by *Neurog2* and *Neurog1*. We show here that transgenic mice expressing a Zeb1/2 dominant-negative form (DBZEB) exhibit reduced numbers of nociceptors and altered pain sensitivity. This reflects an early impairment of *Neurog1*-dependent neurogenesis due to the depletion of specific sensory precursor pools, which is slightly later partially compensated by the contribution of boundary cap cells (BCCs). Indeed, combined *DBZEB* expression and genetic BCCs ablation entirely deplete second wave precursors and, in turn, nociceptors, thus recapitulating the *Neurog1*$^{-/-}$ neuronal phenotype. Altogether, our results uncover roles for Zeb family members in the developing DRGs; they show that the *Neurog1*-dependent sensory neurogenesis can be functionally partitioned in two successive phases; and finally, they illustrate plasticity in the developing peripheral somatosensory system supported by the BCCs, thereby providing a rationale for sensory precursor diversity.

INTRODUCTION

The multiple sensory neuron subtypes of the dorsal root ganglia (DRG) arise from neural crest cells (NCCs) that migrate and differentiate in tightly temporally and spatially regulated phases. In mice, NCCs dedicated to the DRGs leave the neural tube between embryonic day (E)9 and E10 (Serbedzija et al., 1990) and differentiate in two main, partially overlapping, neurogenic waves respectively controlled by the proneural activity of the bHLH transcription factors Neurog2 and Neurog1. Between E9.5 and E11.5 the first *Neurog2*-dependent wave generates Ret-positive(+) and/or TrkB$^+$ and/or TrkC$^+$ mechano- and proprioceptors as well as large diameter TrkA$^+$ neurons (lTrkA). The second *Neurog1*-dependent wave occurs between E10.5 and E13.5 and produces few TrkB$^+$ and TrkC$^+$ neurons as well as small diameter thermonociceptive neurons, which all express TrkA at early stages (sTrkA) and subsequently diverge into "TrkA$^+$ peptidergic" and "Ret$^+$ non-peptidergic" nociceptors (Lawson and Biscoe, 1979; Frank and Sanes, 1991; Ma et al., 1999; Marmigère and Ernfors, 2007; Bourane et al., 2009; Bachy et al., 2011; Lallemend and Ernfors, 2012; Figure S3A). Studies in chick embryos have revealed that second wave precursors form a heterogeneous population (George et al., 2007, 2010). In line with this, boundary cap cells (BCCs) which are involved in structuring spinal nerve roots (Vermeren et al., 2003), have been shown by lineage studies to also directly contribute to about 5% of nociceptors, as well as satellite cells of the mouse DRGs (Maro et al., 2004). It is proposed that BCCs represent a reservoir of neural precursors, an issue supported by their stem cell like properties in vitro (Hjerling-Leffler et al., 2005), but so far hardly assessed in physiopathological conditions in vivo. Here, we addressed the collective roles of Zeb1 and Zeb2 in the early phases of DRG formation. Both proteins form a small family of transcription factors harboring two zinc-finger domains and a homeodomain, involved in many key developmental and physiopathological processes, including epithelio-mesenchymal transitions and the formation of NCCs-derived tissues (Gheldof et al., 2012). Although present in the developing DRGs (Darling et al., 2003; Bassez et al., 2004; Van de Putte et al., 2007; see also Figure S2), their function remains largely unknown. Because of potential functional redundancy, we generated a transgenic mouse model conditionally expressing the first zinc finger domain of the Human ZEB1 protein (hereafter referred to as DBZEB; Sabourin et al., 2009), known to counteract Zeb1 and Zeb2 activity in vitro (Postigo and Dean, 1997). We report that induction of *DBZEB* in NCCs specifically impairs the onset of the second *Neurog1*-dependent sensory neurogenic wave due to the early death of specific precursor pools. This notably leads to drastic, albeit not complete, depletion of nociceptors and altered pain sensitivity in adulthood. We also show that this initial defect of the *Neurog1*-dependent neurogenesis is slightly later partially compensated by the BCCs. Indeed, combined *DBZEB* expression and genetic BCCs ablation lead to complete depletion of second wave precursors and, in turn, of nociceptors, fully recapitulating the *Neurog1*$^{-/-}$ phenotype.

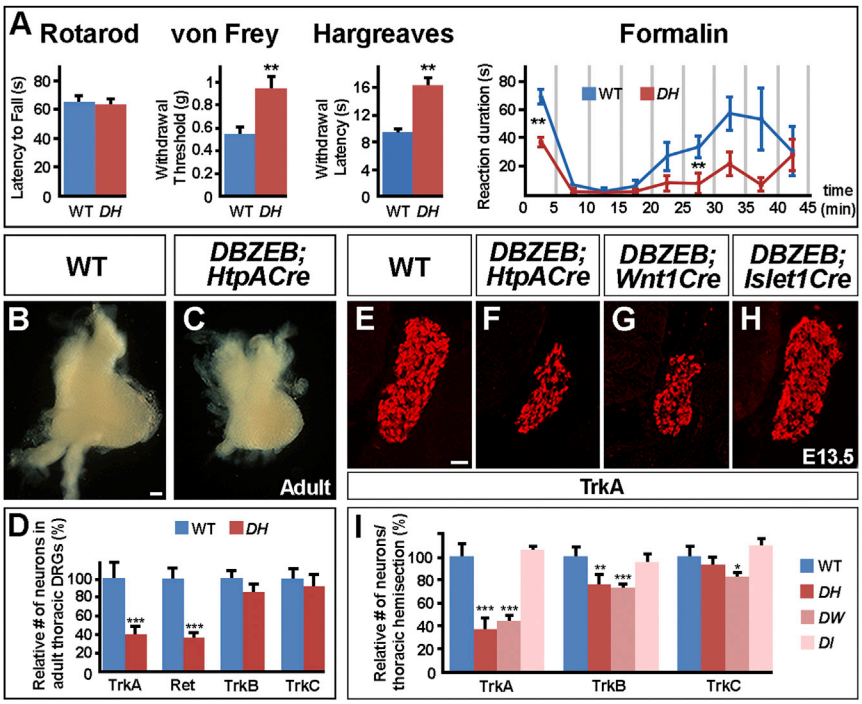

Figure 1. Impaired Response to Noxious Stimuli of *DBZEB;HtpACre* Mice Correlates with Reduced Numbers of Sensory Nociceptors

(A) Rotarod test, mechanical (von Frey), thermal (Hargreaves), and chemical (formalin) nociceptive tests performed on wild-type (WT) and *DBZEB;HtpACre* (*DH*) adults, showing reduced pain sensitivity in transgenic mice. It is of note that both acute and late phase responses to formalin injection were significantly decreased in transgenic animals. Data are represented as mean ± SEM and $^{**}p < 0.01$.

(B and C) Representative images of WT (B) and *DBZEB;HtpACre* (*DH*) (C) adult thoracic DRGs.

(D) Relative quantification of Trk^+ and Ret^+ neurons in adult thoracic DRGs from WT and *DBZEB;HtpACre* (*DH*) animals. Data are represented as mean ± SEM and $^{***}p < 0.001$.

(E–H) Immunofluorescent staining for TrkA on transverse thoracic DRG sections of E13.5 WT (E), *DBZEB;HtpACre* (*DH*) (F), *DBZEB;Wnt1Cre* (G), and *DBZEB;Islet1Cre* (H) embryos.

(I) Relative quantification of Trk^+ neurons in thoracic DRGs from E13.5 WT, *DBZEB;HtpACre* (*DH*), *DBZEB;Wnt1Cre* (*DW*), and *DBZEB;Islet1Cre* (*DI*) embryos. $TrkA^+$ neurons are greatly reduced in *DH* (−63% ± 9%) and *DW* (−55% ± 5%), but not in *DI* embryos. $TrkB^+$ (−25% ± 8%) and both $TrkB^+$ (−28% ± 1.5%) and $TrkC^+$ (−17% ± 4.5%) neurons were also significantly reduced in *DH* and *DW* embryos, respectively.

Data are represented as mean ± SEM; $^{***}p < 0.001$; $^{**}p < 0.01$; and $^{*}p < 0.05$. Scale bars, 50 μm. See also Figure S1.

This illustrates in vivo the participation of the BCCs in ensuring developmental plasticity of the somatosensory system, notably for nociceptive neuron formation.

RESULTS AND DISCUSSION

Impaired Sensitivity of Adult *DBZEB;HtpACre* Mice to Noxious Stimuli Reflects Reduced Numbers of Sensory Nociceptive Neurons

First, we tested whether induction of *DBZEB* in the peripheral nervous system triggered some of the phenotypes reported in *Zeb* knockout mice. Notably, $Zeb2^{cKO/cKO}$*;Wnt1Cre* embryos exhibit developmental defects in the enteric and sympathetic systems (Van de Putte et al., 2007) that we also observed in *DBZEB;Wnt1Cre* animals (Figure S1). This shows that DBZEB is a potent blocker of at least some aspects of Zeb activity also in vivo, thus establishing the *DBZEB* transgenic line as a malleable model to study roles of *Zeb1* and *Zeb2* and their associated human diseases: Polymorphous posterior corneal dystrophy type 3 and Mowat-Wilson syndrome, respectively. Interestingly, some *ZEB1* and *ZEB2* mutations reported in patients possibly produce truncated proteins, which may act as dominant-negative (Krafchak et al., 2005; Mowat et al., 2003).

Because *Zeb2* is involved in vagal NCCs delamination (Van de Putte et al., 2007), to assess *Zeb* function in the forming DRGs, we primarily used the *HtpACre* line, which drives *Cre* expression in post-emigrating NCCs (Pietri et al., 2003). Adult *DBZEB; HtpACre* mice are viable, allowing behavioral studies. In contrast to the rotarod test, during which transgenic animals behaved normally, thus revealing no major motor deficits, in classical mechanical (von Frey assay), thermal (Hargreaves assay), and chemical (formalin assay) nociceptive tests, they exhibited significant reduced pain sensitivity (Figure 1A). A rough anatomical evaluation of the DRGs revealed an obvious size reduction in transgenic mice, particularly at thoracic levels (Figures 1B and 1C). Expression analyses of Ret and Trk receptors showed that while mechano- and proprioceptive neurons were present in close to normal numbers at this stage, there was a reduction of about 60% of both $TrkA^+$ and Ret^+ nociceptive populations in *DBZEB;HtpACre* mice (Figure 1D). At more caudal levels, this phenotype was milder although nociceptors were reduced by 40% (data not shown). These findings are reminiscent of the impaired sensitivity of *Zeb2* heterozygous mice to thermal- and formalin-induced pain (but not mechanical pain) due to altered ion channel expression and slight reduction of nociceptor numbers (Jeub et al., 2011; Pradier et al., 2014). While these data further reinforce the reliability of DBZEB effects, they also show that *DBZEB* expression triggers a stronger phenotype than removing only one allele of *Zeb2*, likely explaining why mechanical pain is also affected in our model.

To determine the etiology of these defects, we analyzed embryonic stages, focusing on thoracic levels. At E13.5, when sensory neurogenesis is nearly complete, we already observed a 63% reduction (±9%) of $sTrkA^+$ nociceptors in *DBZEB;HtpACre* embryos (Figures 1E, 1F, and 1I). Interestingly, we found similar results in *DBZEB;Wnt1Cre* animals (Figures 1G and 1I), demonstrating that induction of *DBZEB* in pre-migrating NCCs does not cause a general failure of delamination, but rather alters specific populations. It is of note that at this stage, $TrkB^+$ and both $TrkB^+$ and $TrkC^+$ populations were also slightly reduced in *DBZEB; HtpACre* and *DBZEB;Wnt1Cre* embryos, respectively (Figure 1I), a discrepancy likely due to differences in timing and/or levels of

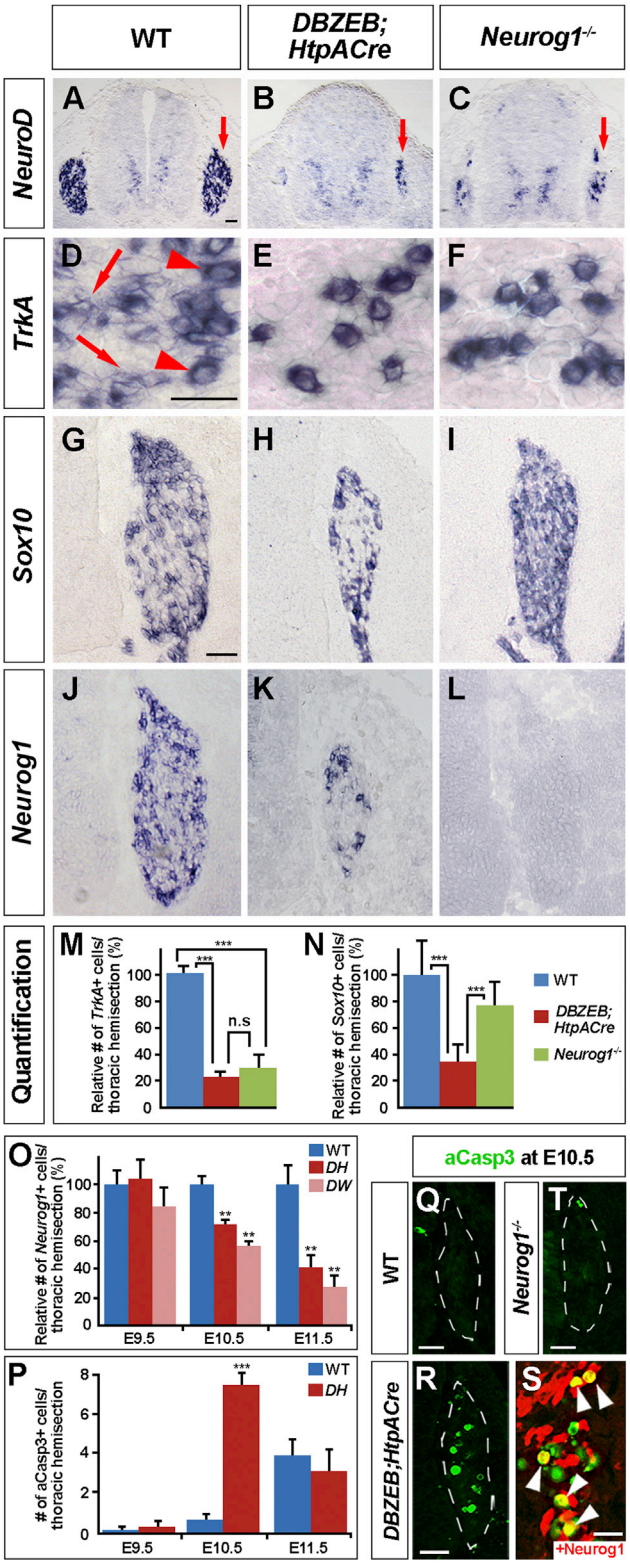

Figure 2. Impaired Onset of the Second Sensory Neurogenic Wave in *DBZEB;HtpACre* Embryos Is Linked to Depletion of *Neurog1*$^+$ Precursors

(A–L) In situ hybridization on transverse thoracic sections of E11.5 WT (A, D, G, and J), *DBZEB;HtpACre* (*DH*) (B, E, H, and K), and *Neurog1*$^{-/-}$ (C, F, I, and L) embryos using *NeuroD* (A–C), *TrkA* (D–F), *Sox10* (G–I), and *Neurog1* (J–L) probes. Arrows in (A)–(C) point toward *NeuroD*$^+$ cells in the DRGs that are similarly reduced in *DBZEB* transgenic embryos and *Neurog1*$^{-/-}$ mutants. (D)–(F) are high magnifications of DRG sections showing large (arrowheads) and small (arrows) *TrkA*$^+$ neurons in WT, while only large *TrkA*$^+$ neurons in *DH* and *Neurog1*$^{-/-}$ embryos.

(M and N) Relative quantification of *TrkA*$^+$ neurons (M) and *Sox10*$^+$ cells (N) in WT, *DBZEB;HtpACre* (*DH*), and *Neurog1*$^{-/-}$ embryos at E11.5. Data are represented as mean ± SEM; ***$p < 0.001$; and not significant (n.s.).

(O) Relative quantification of *Neurog1*$^+$ cells between E9.5 and E11.5 at thoracic levels of WT, *DBZEB;HtpACre* (*DH*), and *DBZEB;Wnt1Cre* (*DW*) embryos. Data are represented as mean ± SEM; **$p < 0.01$; and ***$p < 0.001$.

(P) Quantification of activated Casp3$^+$ (aCasp3$^+$) cells in the DRG anlage of WT and *DBZEB;HtpACre* (*DH*) embryos between E9.5 and E11.5. Data are represented as mean ± SEM and ***$p < 0.001$.

(Q–T) Immunofluorescent staining for aCasp3 alone (Q, R, and T) or combined with Neurog1 (S) on transverse DRG sections of E10.5 WT (Q), *DBZEB;HtpACre* (*DH*) (R and S), and *Neurog1*$^{-/-}$ (T) embryos, showing many apoptotic figures specifically in *DH* mice, some of which being Neurog1$^+$ (arrowheads in S).

See also Figure S2. Scale bars, 25 μm in (S) and 50 μm elsewhere.

Cre expression. The fact that TrkB$^+$ neurons were not significantly affected at adult stages in *DBZEB;HtpACre* mice may possibly reflect a "normalizing effect" of the period of naturally occurring sensory neuron death. Finally, we also found that specific *DBZEB* induction in post-mitotic neurons using the *Islet1Cre* line did not alter the integrity of the DRGs at E13.5 (Figures 1H and 1I), suggesting early requirements of Zeb1/2 proteins at the precursor level.

Impaired Onset of the Second Sensory Neurogenic Wave in *DBZEB* Transgenic Embryos Is Linked to Depletion of Specific *Neurog1*$^+$ Precursor Populations

The early neuronal depletion triggered by DBZEB was reminiscent of some features of the *Neurog1*$^{-/-}$ mutant phenotype (Ma et al., 1999; see also Figures 4S, 4V, and 4W), which prompted us to assess the neurogenic waves of the forming DRGs (Figure S3A). As predicted by the relatively mild alteration of TrkB$^+$ and TrkC$^+$ populations, analyses of *DBZEB;HtpACre* embryos at E9.5 and E10.5 revealed that the first *Neurog2*-dependent neurogenesis occurred largely normally in these animals (Figures S3B–S3G'). In contrast, in E11.5 *DBZEB;HtpACre* embryos, at the peak of the second neurogenic wave, we found altered expression of the neuronal differentiation marker *NeuroD* (Figures 2A and 2B), strikingly comparable to *Neurog1*$^{-/-}$ mutants (Figure 2C), in which residual *NeuroD*$^+$ cells reflect the last neurons issued from the first *Neurog2*-dependent wave (Ma et al., 1999). In line with this, there was an equal reduction of about 70% of the overall *TrkA*$^+$ population in both genetic backgrounds at this stage, specifically affecting the s*TrkA*$^+$ neurons (Figures 2D–2F and 2M). This shows that the onset of the second neurogenic wave is specifically impaired in *DBZEB* transgenic mice. Furthermore, we concomitantly found a 65% reduction (±12%) of *Sox10*$^+$ precursors in *DBZEB;HtpACre* embryos (Figures 2G, 2H, and 2N), in contrast to *Neurog1*$^{-/-}$ mutants, in which close to normal numbers of *Sox10*$^+$ cells were still present at this stage (Figures 2I and 2N) and rather diminished subsequently (data not shown). This reveals that at the precursor level *DBZEB;HtpACre* embryos exhibit a stronger phenotype than *Neurog1*$^{-/-}$ mutants at E11.5. Moreover, time course analysis of *Neurog1* expression

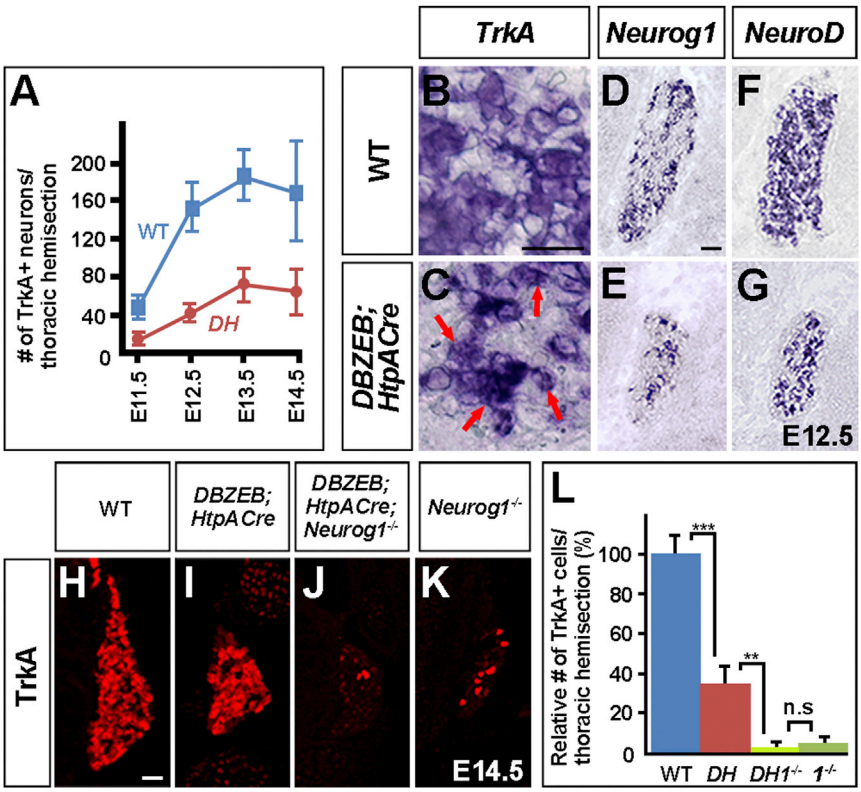

Figure 3. Partial Recovery of Nociceptors in *DBZEB;HtpACre* Embryos from E12 Is *Neurog1* Dependent

(A) Time course analysis of *TrkA*$^+$ neurons from E11.5 to E14.5 in WT and *DBZEB;HtpACre* (*DH*) embryos.

(B–G) Data are represented as mean ± SEM. In situ hybridization on transverse thoracic DRG sections from WT (B, D, and F) and *DH* (C, E, and G) embryos at E12.5, using *TrkA* (B and C), *Neurog1* (D and E), and *NeuroD* (F and G) probes. (B) and (C) are high magnifications showing the presence of s*TrkA*$^+$ neurons in transgenic animals at this stage (arrows in C).

(H–K) Immunofluorescent staining for TrkA on transverse thoracic DRG sections from E14.5 WT (H), *DBZEB;HtpACre* (I), *DBZEB;HtpACre; Neurog1*$^{-/-}$ (J), and *Neurog1*$^{-/-}$ (K) embryos.

(L) Relative quantification of TrkA$^+$ neurons in WT, *DBZEB;HtpACre* (*DH*), *DBZEB;HtpACre; Neurog1*$^{-/-}$ (*DH1*$^{-/-}$), and *Neurog1*$^{-/-}$ (*1*$^{-/-}$). Data are represented as mean ± SEM; *p < 0.001; and not significant (n.s.). Scale bars, 50 μm.

revealed that the primary phase of *Neurog1* expression in first wave precursors initiated at E9.5 under the control of Neurog2 (Figure S3A; Ma et al., 1999) was normal in transgenic embryos (Figures 2O, S3D, and S3D'). At E10.5, although many *Neurog1*$^+$ and *NeuroD*$^+$ cells were still observed, reflecting the ongoing first neurogenic wave (Figures S3F and S3G'), we already found a 28% (±3%) reduction of the *Neurog1*$^+$ population (Figure 2O), which reached 62% (±7%) at E11.5 (Figures 2J, 2K, and 2O), thus paralleling the diminution of *Sox10*$^+$ cells (Figures 2G, 2H, and 2N). These data, together with the described roles of Zeb proteins in neural cell survival (Ohayon et al., 2009; Sabourin et al., 2009; Miquelajauregui et al., 2007), prompted us to assess cell death. Time course analysis of the apoptosis marker "activated Caspase-3" (aCasp3) between E9.5 and E11.5 revealed a massive increase of dying cells specifically in the DRG anlage of *DBZEB;HtpACre* embryos at E10.5 (Figures 2P–2R), some of which being Neurog1$^+$ (Figure 2S). It is of note that *DBZEB;Wnt1Cre* embryos exhibited similar phenotypes (Figures 2O, S3B"–S3G", and S3H–S3K), although at E10.5 numbers of *Neurog1*$^+$ precursors were already reduced by 43% (±4%; Figure 2O), likely due to temporal and spatial divergences in apoptosis induction. Indeed, in these animals, we observed dying cells at E9.5 and E10.5, which were mainly located in the roof of the neural tube (Figures S3M–S3O'). Thus, these results indicate that alteration of *Neurog1* expression in *DBZEB;HtpACre* and *DBZEB;Wnt1Cre* mice at E11.5 is the consequence, and not the cause, of increased apoptosis of second wave precursors, also supported by the absence of dying cells in *Neurog1*$^{-/-}$ mutants at E10.5 (Figure 2T).

Altogether, these data show that induction of DBZEB in pre- or post-emigrating NCCs leaves largely intact first wave precursors undergoing the *Neurog2*-dependent neurogenesis and instead specifically affects the integrity of second wave precursor pools, leading to impaired onset of the *Neurog1*-dependent neurogenic wave. These early effects are consistent with Zeb expression profiles in the developing DRGs. Nevertheless, while all Pax3$^+$ NCCs, including Neurog2$^+$ and Neurog1$^+$ sensory precursors, express Zeb2 from E9.5, they display no or low levels of Zeb1, which is rather upregulated in Islet1$^+$ post-mitotic neurons (Figure S2). It is thus likely that the phenotypes triggered by DBZEB mainly reflect alteration of *Zeb2* function.

Partial Recovery of Nociceptors in *DBZEB* Transgenic Mice Is *Neurog1* Dependent

Intriguingly, virtual absence of *sTrkA*$^+$ neurons at thoracic levels of E11.5 *DBZEB;HtpACre* and *DBZEB;Wnt1Cre* animals contrasted with their presence at E13.5 (see Figures 1E–1G and 1I). Time course analysis of *TrkA* expression indeed showed that s*TrkA*$^+$ nociceptors first arise at E12 in transgenic embryos and expand afterward, though at a lower rate compared to controls (Figures 3A–3C; data not shown). Consistent with this, we detected *Neurog1*$^+$ precursors and *NeuroD*$^+$ differentiating neurons at E12.5 (Figures 3D–3G), revealing that in contrast to *Neurog1*$^{-/-}$ mutants (Figure 4P; Ma et al., 1999), the second neurogenic wave is not totally blocked in transgenic mice, but is postponed. Furthermore, by analyzing *DBZEB;HtpACre; Neurog1*$^{-/-}$ embryos at E14.5, we found that, unlike *DBZEB; HtpACre* mice, compound mutants exhibited a complete lack of sTrkA$^+$ neurons, like *Neurog1*$^{-/-}$ mutants (Figures 3H–3L). These data thus show that the initial impairment of nociceptor production in *DBZEB;HtpACre* embryos is slightly later partially compensated through a *Neurog1*-dependent mechanism.

Combined *DBZEB* Expression and Genetic BCC Ablation Lead to Entire Depletion of Second Wave Precursors and Recapitulate the *Neurog1*$^{-/-}$ Neuronal Phenotype

Obviously, a pool of sensory precursors undergoing the *Neurog1*-dependent neurogenesis appeared insensitive to DBZEB. BCCs emerged as good candidates to participate in this apparent compensatory process since the first sign of their differentiation is the induction of *Egr2* at E10.75, after the second neurogenic wave has normally started, and the first BCC-derived neurons arise at E12 (Maro et al., 2004). We first assessed the status of BCCs in *DBZEB* transgenic mice using the *Egr2*^{LacZ} allele. On whole mount preparations of *DBZEB;HtpACre;Egr2*$^{LacZ/+}$ embryos at E12, we observed reduced numbers of BCCs all along the anteroposterior axis (Figures 4A and 4C). According to Zeb2 (but not Zeb1) expression in BCCs (Figures S2S and S2T), this might reflect a direct implication in their development. Nevertheless, on dissected DRGs, in contrast to controls in which X-Gal^{+} cells were confined around spinal nerve roots (arrows in Figures 4B and 4D), in transgenic mice, we intriguingly observed X-Gal staining inside the DRGs (arrowhead in Figure 4D). In line with this, on sections we occasionally detected ectopic *Egr2*$^{+}$ cells in the DRGs of *DBZEB;HtpACre* embryos at E12 (Figures 4E–4H; see also S3L), some of which being *TrkA*$^{+}$ (arrowheads in Figure 4H). Therefore, another possible non-mutually exclusive explanation to the reduced numbers of BCCs is that, as a consequence of sensory precursor loss, these cells abnormally colonize the DRG anlage of *DBZEB* transgenic mice. These observations further prompted us to directly assess whether *Egr2*$^{+}$ BCCs indeed support the recovery of nociceptors in these animals. To test this, we took advantage of the *Egr2*^{DT} allele (Vermeren et al., 2003) and mainly used *Wnt1Cre*, which, in our hands, was more efficient in triggering BCCs ablation than *HtpACre* (data not shown). First, studies of *Wnt1Cre;Egr2*$^{DT/+}$ embryos confirmed that at E13.5 there was a 55% (±5%) reduction of nociceptors (Figures S4A–S4C; Maro et al., 2004), as well as a slight reduction of both TrkB^{+} and TrkC^{+} populations (−18% ± 2% and −12% ± 1.5%, respectively; Figure S4C). In addition, analyses at E11.5 revealed that while the second neurogenic wave was initiated at the right time in these animals, as illustrated by the presence of many *NeuroD*$^{+}$ and s*TrkA*$^{+}$ cells (Figures S4D–S4G), there was a concomitant 50% reduction of *Sox10*$^{+}$ and *Neurog1*$^{+}$ precursors (Figures S4H–S4K; quantified in 4K). These results show that BCCs ablation leads to the depletion of a *Neurog1*$^{+}$ precursor pool as early as E11.5 that appeared strikingly complementary to that observed in *DBZEB* transgenic mice. We next analyzed *DBZEB;Wnt1Cre;Egr2*$^{DT/+}$ compound transgenic embryos and found that, as early as E11.5, there was a virtual complete loss of *Neurog1*$^{+}$ precursors at thoracic levels (Figures 4I–4K), paralleled by a drastic reduction of *Sox10*$^{+}$ cells, the remaining ones typically lying around the DRG anlage and likely constituting glial precursors (Figures 4L and 4M). Consistent with this, from E12, complete absence of *NeuroD*$^{+}$ differentiating neurons in compound transgenic mice demonstrated that the second sensory neurogenic wave was totally impaired, fully mimicking the *Neurog1*$^{-/-}$ phenotype (Figures 4N–4P). In line with this, comparative analyses of *DBZEB;Wnt1Cre;Egr2*$^{DT/+}$ and *Neurog1*$^{-/-}$ embryos at E13.5 revealed similar neuronal phenotypes at thoracic levels, including a virtual absence of sTrkA^{+} nociceptors and reduction of about 25% of both TrkB^{+} and TrkC^{+} populations (Figures 4Q–4W; Ma et al., 1999). These results thus demonstrate complementary deleterious effects of *DBZEB* expression and BCCs ablation on DRG formation, leading to an entire depletion of second wave *Neurog1*$^{+}$ precursors, and in turn, notably to complete agenesis of nociceptive neurons. They also demonstrate that BCCs indeed participate in the recovery of nociceptors observed in *DBZEB* transgenic mice.

Taken together, our data illustrate the complex and dynamic events ensuring the formation of the peripheral somatosensory system. Using a dominant-negative approach, we uncover roles of Zeb family members in this system, most likely attributable to Zeb2 according to expression profile analyses. Although Zeb2 is a general marker of first and second wave precursors, including BCCs, *DBZEB* induction in pre- or post-emigrating NCCs leaves largely intact the first *Neurog2*-dependent neurogenic wave and instead affects the onset of the second *Neurog1*-dependent neurogenesis, as the consequence of the early depletion of specific sensory precursor populations. This notably leads to drastic, albeit not complete, reduction of nociceptors, thus giving an explanation for the altered pain sensitivity observed in adult transgenic animals. The reason for this partial requirement remains unclear, but supports the view that peripheral somatosensory precursors are heterogeneous (Frank and Sanes, 1991; Ma et al., 1999; George et al., 2007, 2010; Maro et al., 2004). In line with this, combined effects of *DBZEB* expression and genetic BCCs ablation, which recapitulate the *Neurog1*$^{-/-}$ phenotype, establish that the *Neurog1*-dependent neurogenesis can be functionally partitioned in at least two consecutive phases involving distinct precursor populations with specific developmental modalities: a first pool is *Zeb*-dependent and differentiates from E10.5; a second pool is BCCs-dependent and differentiates slightly later. We also refine the requirement of BCCs in the forming DRGs by revealing that reduced numbers of nociceptors previously reported in embryos devoid of BCCs (Maro et al., 2004) reflect, at least in part, an early depletion of precursor cells. We also present genetic evidences that in a context of early nociceptive precursor loss triggered here by DBZEB, BCCs have the capacity to support the formation of significant numbers of nociceptors, which correlates with the presence of ectopic *Egr2*$^{+}$ cells in the DRGs of *DBZEB* transgenic mice. Finally, altogether, our data illustrate that Zeb family members and BCCs underlie developmental plasticity of nociceptive neurons, thereby providing a rationale for somatosensory precursor diversity.

EXPERIMENTAL PROCEDURES

Mouse Strains

Procedures involving animals and their care were conducted according to the French Ministry of Agriculture and the European Community Council Directive no. 86/609/EEC, OJL 358. Protocols were validated by the Direction Départementale des Services Vétérinaires de l'Hérault (Certificate of Animal Experimentation no. 34-376). *DBZEB* (Sabourin et al., 2009), *HtpACre* (Pietri et al., 2003), *Wnt1Cre* (Danielian et al., 1998), *Islet1Cre* (Srinivas et al., 2001), *Neurog1* (Ma et al., 1999), *Egr2*^{LacZ} (Maro et al., 2004), and *Egr2*^{GFPDT} (Vermeren et al., 2003) mouse strains were used in this study.

Behavioral Tests

Experiments were performed blindly on groups of at least six males and females from wild-type and *DBZEB;HtpACre* genotypes.

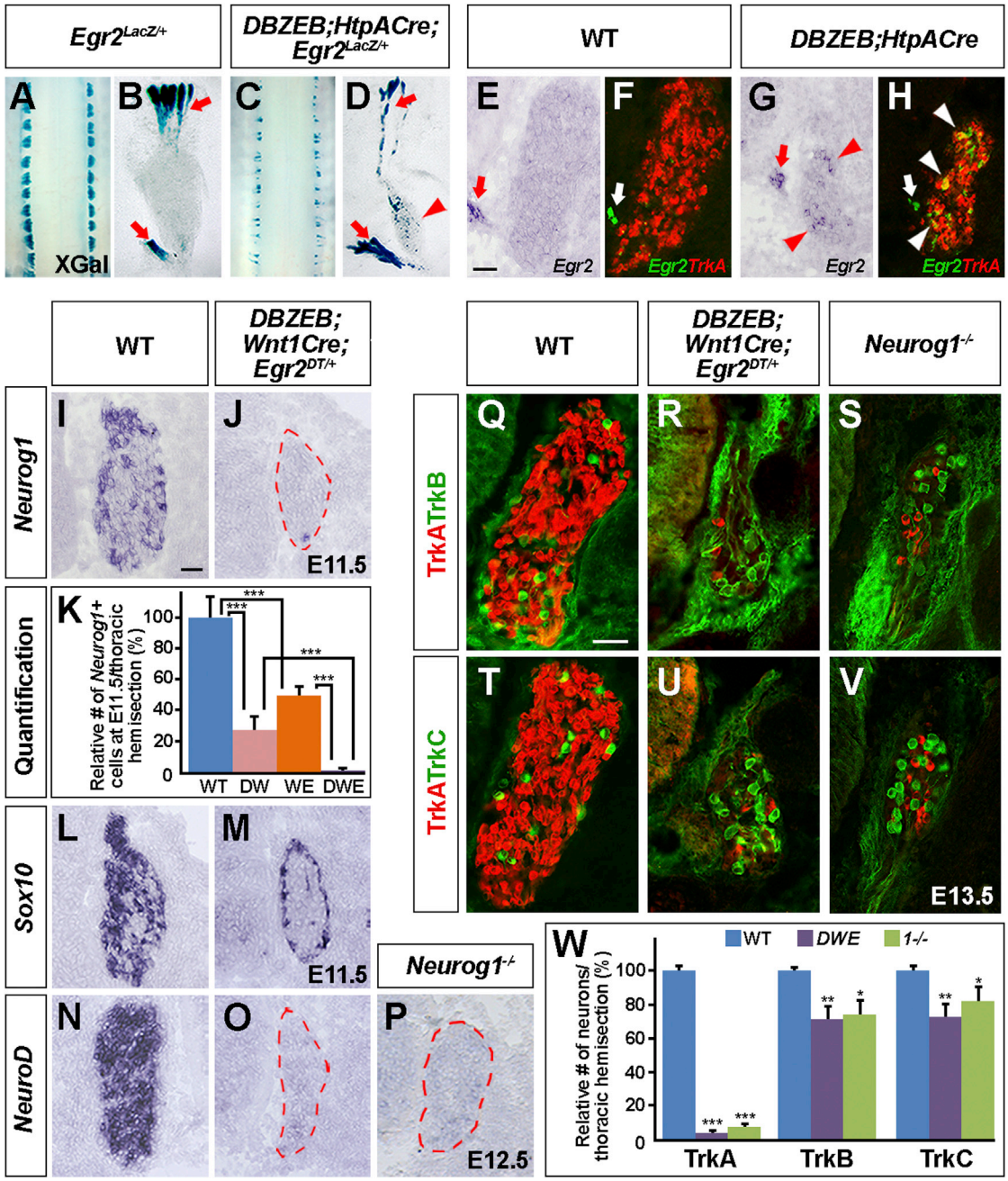

Figure 4. Combined *DBZEB* Expression and BCC Ablation Lead to Entire Depletion of Second Wave Precursors and Recapitulate the *Neurog1*$^{-/-}$ Neuronal Phenotype

(A–D) X-Gal staining on E12 *Egr2*$^{LacZ/+}$ (A and B) and *DBZEB;HtpACre;Egr2*$^{LacZ/+}$ (C and D) embryos. (A) and (C) are dorsal views of whole embryos. (B) and (D) show representative images of dissected DRGs. Arrows point toward the BCCs, while arrowhead points toward ectopic X-Gal^{+} cells inside the DRGs of *DBZEB;HtpACre;Egr2*$^{LacZ/+}$ mice.

(E–H) In situ hybridization using an *Egr2* probe alone (E and G) or combined with a *TrkA* probe (F and H) on transverse thoracic DRG sections of E12 WT (E and F) and *DBZEB;HtpACre* (*DH*) (G and H) embryos. Arrows point toward *Egr2*$^{+}$ BCCs, while arrowheads point toward ectopic *Egr2*$^{+}$ cells in the DRGs of *DH* animals, some of which being *TrkA*$^{+}$ (H).

(I and J) In situ hybridization on transverse thoracic DRG sections from E11.5 WT (I) and *DBZEB;Wnt1Cre;Egr2*$^{DT/+}$ (J) embryos using a *Neurog1* probe.

(K) Compilation of the relative numbers of *Neurog1*$^{+}$ cells in thoracic DRGs of E11.5 WT, *DBZEB;Wnt1Cre* (*DW*), *Wnt1Cre;Egr2*$^{DT/+}$ (*WE*), and *DBZEB; Wnt1Cre;Egr2*$^{DT/+}$ (*DWE*) embryos. Data are represented as mean ± SEM and ***$p < 0.001$.

(L–P) In situ hybridization on transverse thoracic DRG sections from WT (L and N), *DBZEB;Wnt1Cre;Egr2*$^{DT/+}$ (M and O), and *Neurog1*$^{-/-}$ (P) embryos at E11.5 (L and M) or E12.5 (N–P) using *Sox10* (L and M) and *NeuroD* (N–P) probes.

(legend continued on next page)

Motor Activity

Mice were trained on the Rotarod apparatus at a fixed speed of 10 rotations per minute (rpm) for 2 consecutive days. They were then tested for the acceleration task, during which the speed progressively increased from 4 to 40 rpm over a 5 min period. The latency to fall was recorded. Data were analyzed by unpaired t test.

Tactile Sensitivity

Paw-withdrawal thresholds of the hindpaw were determined in response to probing with calibrated von Frey filaments ranging from 0.4 to 4.0 grams (g). Mice were allowed to acclimate in suspended wire-mesh cages for 1 hr. Each filament was applied perpendicularly to the plantar surface of the paw. Withdrawal thresholds were determined by sequentially increasing and decreasing the stimulus strength ("up and down" method). Data were analyzed using a Dixon non-parametric test and expressed as the mean withdrawal threshold. Unpaired t test was used for statistical analysis.

Heat Sensitivity

The method of Hargreaves (Hargreaves et al., 1988) was used to assess paw-withdrawal latency to a thermal nociceptive stimulus. Mice were allowed to acclimate in a Plexiglas enclosure on a clear glass plate in a quiet testing room for 1 hr. A radiant heat source (a high-intensity projector lamp) was focused onto the plantar surface of the paw. Paw-withdrawal latency was determined. Each paw was tested three times with a 10 min interval between each trial. A maximal cutoff time of 20 s was used to prevent tissue damage. Data were analyzed using unpaired t test.

Nocifensive Behavior

Experimental animals underwent treatment with formalin. Briefly, animals were subjected to intraplantar injections of sterile 2.5% formalin (10 μl) just under the skin on the dorsal surface of the hindpaw. Pain responses (licking and biting) were recorded for a period of 45 min by 5 min intervals. Data were analyzed by *repeated-measures ANOVA* followed by Dunnett's test.

In Situ Hybridization, Immunofluorescence, and X-Gal Staining

Single or double in situ hybridization experiments and immunofluorescent staining were performed as previously described (Bourane et al., 2009). Antisense RNA probes for *DBH*, *Egr2*, *NeuroD*, *Neurog1*, *Neurog2*, *Ret*, *Sox10*, *TrkA*, *TrkB*, and *TrkC* were labeled using the DIG or Fluorescein RNA labeling kits (Roche). Primary antibodies used in this study were as follows: chicken anti-GFP (Abcam); goat anti-Neurog1 (Santa Cruz), Neurog2 (Santa Cruz), TrkB (R&D Systems), and TrkC (R&D Systems); mouse anti-Islet1/2 (Developmental Studies Hybridoma Bank [DSHB]) and Pax3 (DSHB); and rabbit anti-aCasp3 (Cell Signaling), TrkA (Millipore), Zeb1 (Darling et al., 2003), and Zeb2 (Santa Cruz). X-Gal staining was performed as described (Knittel et al., 1995).

Cell Counts

Quantitative analyses were carried out on at least four independent animals from each genotype. DRGs sections were imaged using a Zeiss microscope, and cell counts were performed using the Image J software. Data were statistically analyzed using Student's t test and represented as mean ± SEM.

SUPPLEMENTAL INFORMATION

Supplemental Information includes four figures and can be found with this article online at http://dx.doi.org/10.1016/j.devcel.2015.03.021.

AUTHOR CONTRIBUTIONS

D.O., S.V., P.A.L., C.S., and A.P. performed the experiments. A.G., C.R., J.V., P.C., P.T., and A.P. designed and supervised the experiments and interpreted the data. C.R. participated in the writing. A.P. wrote the manuscript.

ACKNOWLEDGMENTS

We thank W. Joly for critical reading of the manuscript, S. Mallié for technical help, and the staff of the animal house of the Institut des Neurosciences de Montpellier (INM). We also thank S. Arber, J.F. Brunet, D. Darling, S. Dufour, C. Goridis, D. Grégoire, F. Guillemot, T. Jessell, and A. McMahon for the kind gift of mouse strains and materials. This work was funded by INSERM, CNRS, Association Française contre les Myopathies (AFM), and Agence Nationale pour la Recherche (ANR05JCJC00590).

Received: October 13, 2014
Revised: January 19, 2015
Accepted: March 25, 2015
Published: May 4, 2015

REFERENCES

Bachy, I., Franck, M.C., Li, L., Abdo, H., Pattyn, A., and Ernfors, P. (2011). The transcription factor Cux2 marks development of an A-delta sublineage of TrkA sensory neurons. Dev. Biol. *360*, 77–86.

Bassez, G., Camand, O.J., Cacheux, V., Kobetz, A., Dastot-Le Moal, F., Marchant, D., Catala, M., Abitbol, M., and Goossens, M. (2004). Pleiotropic and diverse expression of ZFHX1B gene transcripts during mouse and human development supports the various clinical manifestations of the "Mowat-Wilson" syndrome. Neurobiol. Dis. *15*, 240–250.

Bourane, S., Garces, A., Venteo, S., Pattyn, A., Hubert, T., Fichard, A., Puech, S., Boukhaddaoui, H., Baudet, C., Takahashi, S., et al. (2009). Low-threshold mechanoreceptor subtypes selectively express MafA and are specified by Ret signaling. Neuron *64*, 857–870.

Danielian, P.S., Muccino, D., Rowitch, D.H., Michael, S.K., and McMahon, A.P. (1998). Modification of gene activity in mouse embryos in utero by a tamoxifen-inducible form of Cre recombinase. Curr. Biol. *8*, 1323–1326.

Darling, D.S., Stearman, R.P., Qi, Y., Qiu, M.S., and Feller, J.P. (2003). Expression of Zfhep/deltaEF1 protein in palate, neural progenitors, and differentiated neurons. Gene Expr. Patterns *3*, 709–717.

Frank, E., and Sanes, J.R. (1991). Lineage of neurons and glia in chick dorsal root ganglia: analysis in vivo with a recombinant retrovirus. Development *111*, 895–908.

George, L., Chaverra, M., Todd, V., Lansford, R., and Lefcort, F. (2007). Nociceptive sensory neurons derive from contralaterally migrating, fate-restricted neural crest cells. Nat. Neurosci. *10*, 1287–1293.

George, L., Kasemeier-Kulesa, J., Nelson, B.R., Koyano-Nakagawa, N., and Lefcort, F. (2010). Patterned assembly and neurogenesis in the chick dorsal root ganglion. J. Comp. Neurol. *518*, 405–422.

Gheldof, A., Hulpiau, P., van Roy, F., De Craene, B., and Berx, G. (2012). Evolutionary functional analysis and molecular regulation of the ZEB transcription factors. Cell. Mol. Life Sci. *69*, 2527–2541.

Hargreaves, K., Dubner, R., Brown, F., Flores, C., and Joris, J. (1988). A new and sensitive method for measuring thermal nociception in cutaneous hyperalgesia. Pain *32*, 77–88.

Hjerling-Leffler, J., Marmigère, F., Heglind, M., Cederberg, A., Koltzenburg, M., Enerbäck, S., and Ernfors, P. (2005). The boundary cap: a source of neural crest stem cells that generate multiple sensory neuron subtypes. Development *132*, 2623–2632.

Jeub, M., Emrich, M., Pradier, B., Taha, O., Gailus-Durner, V., Fuchs, H., de Angelis, M.H., Huylebroeck, D., Zimmer, A., Beck, H., and Racz, I. (2011). The transcription factor Smad-interacting protein 1 controls pain sensitivity via modulation of DRG neuron excitability. Pain *152*, 2384–2398.

(Q–V) Double immunofluorescent staining for TrkA and TrkB (Q–S) or TrkC (T–V) on transverse thoracic DRG sections of E13.5 WT (Q and T), *DBZEB;Wnt1Cre;Egr2*$^{DT/+}$ (R and U), and *Neurog1*$^{-/-}$ (S and V) embryos.

(W) Relative quantification of TrkA$^+$, TrkB$^+$, and TrkC$^+$ neurons on thoracic hemisections from E13.5 WT, *DBZEB;Wnt1Cre;Egr2*$^{DT/+}$ (*DWE*), and *Neurog1*$^{-/-}$ (*1*$^{-/-}$) revealing similar neuronal depletion in *DBZEB;Wnt1Cre;Egr2*$^{DT/+}$ and *Neurog1*$^{-/-}$ embryos.

Data are represented as mean ± SEM; *$p < 0.05$; **$p < 0.01$; and ***$p < 0.001$. Scale bars, 50 μm. See also Figures S2–S4.

Knittel, T., Kessel, M., Kim, M.H., and Gruss, P. (1995). A conserved enhancer of the human and murine Hoxa-7 gene specifies the anterior boundary of expression during embryonal development. Development *121*, 1077–1088.

Krafchak, C.M., Pawar, H., Moroi, S.E., Sugar, A., Lichter, P.R., Mackey, D.A., Mian, S., Nairus, T., Elner, V., Schteingart, M.T., et al. (2005). Mutations in TCF8 cause posterior polymorphous corneal dystrophy and ectopic expression of COL4A3 by corneal endothelial cells. Am. J. Hum. Genet. *77*, 694–708.

Lallemend, F., and Ernfors, P. (2012). Molecular interactions underlying the specification of sensory neurons. Trends Neurosci. *35*, 373–381.

Lawson, S.N., and Biscoe, T.J. (1979). Development of mouse dorsal root ganglia: an autoradiographic and quantitative study. J. Neurocytol. *8*, 265–274.

Ma, Q., Fode, C., Guillemot, F., and Anderson, D.J. (1999). Neurogenin1 and neurogenin2 control two distinct waves of neurogenesis in developing dorsal root ganglia. Genes Dev. *13*, 1717–1728.

Marmigère, F., and Ernfors, P. (2007). Specification and connectivity of neuronal subtypes in the sensory lineage. Nat. Rev. Neurosci. *8*, 114–127.

Maro, G.S., Vermeren, M., Voiculescu, O., Melton, L., Cohen, J., Charnay, P., and Topilko, P. (2004). Neural crest boundary cap cells constitute a source of neuronal and glial cells of the PNS. Nat. Neurosci. *7*, 930–938.

Miquelajauregui, A., Van de Putte, T., Polyakov, A., Nityanandam, A., Boppana, S., Seuntjens, E., Karabinos, A., Higashi, Y., Huylebroeck, D., and Tarabykin, V. (2007). Smad-interacting protein-1 (Zfhx1b) acts upstream of Wnt signaling in the mouse hippocampus and controls its formation. Proc. Natl. Acad. Sci. USA *104*, 12919–12924.

Mowat, D.R., Wilson, M.J., and Goossens, M. (2003). Mowat-Wilson syndrome. J. Med. Genet. *40*, 305–310.

Ohayon, D., Pattyn, A., Venteo, S., Valmier, J., Carroll, P., and Garces, A. (2009). Zfh1 promotes survival of a peripheral glia subtype by antagonizing a Jun N-terminal kinase-dependent apoptotic pathway. EMBO J. *28*, 3228–3243.

Pietri, T., Eder, O., Blanche, M., Thiery, J.P., and Dufour, S. (2003). The human tissue plasminogen activator-Cre mouse: a new tool for targeting specifically neural crest cells and their derivatives in vivo. Dev. Biol. *259*, 176–187.

Postigo, A.A., and Dean, D.C. (1997). ZEB, a vertebrate homolog of Drosophila Zfh-1, is a negative regulator of muscle differentiation. EMBO J. *16*, 3935–3943.

Pradier, B., Jeub, M., Markert, A., Mauer, D., Tolksdorf, K., Van de Putte, T., Seuntjens, E., Gailus-Durner, V., Fuchs, H., Hrabě de Angelis, M., et al. (2014). Smad-interacting protein 1 affects acute and tonic, but not chronic pain. Eur. J. Pain *18*, 249–257.

Sabourin, J.C., Ackema, K.B., Ohayon, D., Guichet, P.O., Perrin, F.E., Garces, A., Ripoll, C., Charité, J., Simonneau, L., Kettenmann, H., et al. (2009). A mesenchymal-like ZEB1(+) niche harbors dorsal radial glial fibrillary acidic protein-positive stem cells in the spinal cord. Stem Cells *27*, 2722–2733.

Serbedzija, G.N., Fraser, S.E., and Bronner-Fraser, M. (1990). Pathways of trunk neural crest cell migration in the mouse embryo as revealed by vital dye labelling. Development *108*, 605–612.

Srinivas, S., Watanabe, T., Lin, C.S., William, C.M., Tanabe, Y., Jessell, T.M., and Costantini, F. (2001). Cre reporter strains produced by targeted insertion of EYFP and ECFP into the ROSA26 locus. BMC Dev. Biol. *1*, 4.

Van de Putte, T., Francis, A., Nelles, L., van Grunsven, L.A., and Huylebroeck, D. (2007). Neural crest-specific removal of Zfhx1b in mouse leads to a wide range of neurocristopathies reminiscent of Mowat-Wilson syndrome. Hum. Mol. Genet. *16*, 1423–1436.

Vermeren, M., Maro, G.S., Bron, R., McGonnell, I.M., Charnay, P., Topilko, P., and Cohen, J. (2003). Integrity of developing spinal motor columns is regulated by neural crest derivatives at motor exit points. Neuron *37*, 403–415.